JOC The Journal of Organic Chemistry

Article

pubs.acs.org/joc

KuQuinones Equilibria Assessment for Biomedical Applications

Federica Sabuzi,[†] Sara Lentini,[†] Fabio Sforza,[‡] Silvia Pezzola,[†] Silvia Fratelli,[†] Olga Bortolini,[‡] Barbara Floris,[†] Valeria Conte,[†] and Pierluca Galloni*[,†]

[†]Dipartimento di Scienze e Tecnologie Chimiche, Università di Roma "Tor Vergata", Via della Ricerca Scientifica snc, 00133 Rome, Italy

[‡]Dipartimento di Scienze Chimiche e Farmaceutiche, and Dipartimento di Scienze della Vita e Biotecnologie, Università di Ferrara, via Luigi Borsari 46, 44121 Ferrara, Italy

Supporting Information

ABSTRACT: A small library of pentacyclic quinoid compounds, called KuQuinones (KuQs), has been prepared through a one-pot reaction. KuQuinones complex structure is made up by two naphthoquinone units connected by a five-membered ring. Due to KuQs structural features, keto−enol tautomerization in solution likely occurs, leading to the generation of four different species, i.e., the enol, the enolate, the external enol and the diquinoid species. The interchange among KuQ tautomers leads to substantial spectral variations of the dye depending on the experimental conditions used. The comprehension of tautomeric equilibria of this new class of quinoid compounds is strongly required in order to explain their behavior in solution and in biological environment. UV−vis, ^{1}H NMR spectroscopies, and DFT calculations resulted appropriate tools to understand the nature of the prevalent KuQuinone species in solution. Moreover, due to the structural similarity of KuQuinones with camptothecin (CPT), a largely used anticancer agent, KuQs have been tested against Cisplatin-resistant SKOV3 and SW480 cancer cell lines. Results highlighted that KuQs are highly active toward the analyzed cell lines and almost nontoxic for healthy cell, indicating a high specific activity.

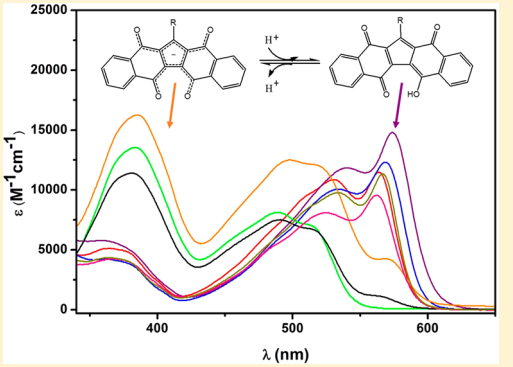

INTRODUCTION

Nowadays the rapid expansion of chemotherapy resistance mechanisms is opening new windows for drugs development and it is attracting a growing number of research groups.[1] Currently, the majority of chemotherapeutic drugs are either natural substances (eventually modified)[1b] or synthetic products, inspired by natural ones. Among them, quinones derivatives have a primary role as antitumor drugs; as an example, *lapachol*,[2] its pyrano and furano naphthoquinone derivatives,[3−7] *shikonin*,[8,9] as well as *doxorubicin*[10] are characterized by the highest and most selective antiproliferative activity toward different human cancer cells and they also exhibit a wide spectrum of anticancer activity.

In 2012, we described a one-pot reaction for the synthesis of a new class of quinoid compounds, called KuQuinones (KuQs).[11] Such compounds are characterized by a pentacyclic skeleton where two naphthoquinoid units are fused with a central five membered ring; similar structure has been found in some natural pigments with interesting sun skin properties.[12] To the best of our knowledge, KuQs synthesis represents a unique case where an entirely conjugated pentacyclic molecule is prepared through a one-pot reaction. Interest in KuQuinones arises from their pentacyclic and conjugated structure that resulted a crucial feature for their application as dye sensitizers in photoelectrochemical devices.[13] Moreover, the structural similarity of 1-ethylKuQuinone (KuQEt) with camptothecin (CPT), topotecan (the water-soluble CPT analogue), and also with other polycyclic anticancer molecules (Figure 1), suggested the potential application of KuQs also as antitumor agents.[14−16]

In this context, the anticancer activity of 1-ethylKuQuinone (KuQEt) has been preliminary investigated and better IC_{50} values than those of *cis*-platinum (CDDP, a common chemotherapeutic drug, used in the treatment of different cancers), together with lower side effects on healthy cells, were detected on SKOV3 and SW480 lines, established for ovarian and colon pathologies.[11] As for CPT,[17,18] it has been demonstrated that KuQEt interacts with human topoisomerase I (TopI) but with a different mechanism: KuQEt is able to inhibit the cleavage of the DNA strand and consequently to induce cell death.[19] Additionally, previous studies highlighted that KuQEt showed negligible cytotoxicity on healthy human fibroblasts (HF).

To further understand the KuQs species involved in the formation of the DNA-TopI complex inside the cells, a detailed study of KuQuinones equilibria in solution is however necessary; to this aim, the synthesis of a new KuQuinone

Received: June 28, 2017
Published: September 5, 2017

DOI: 10.1021/acs.joc.7b01602
J. Org. Chem. XXXX, XXX, XXX−XXX

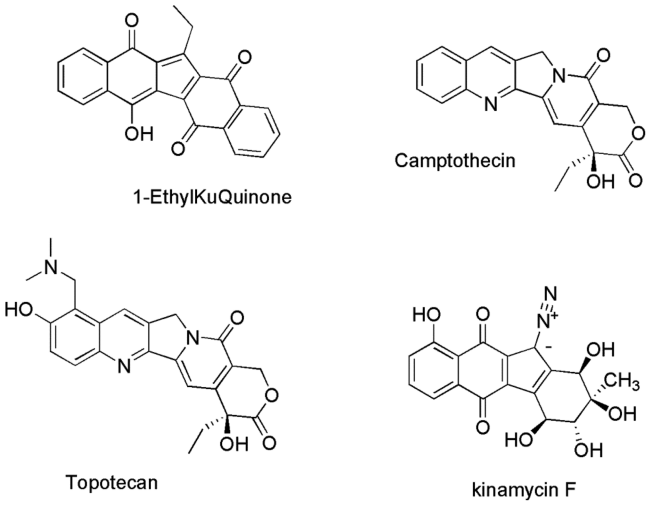

Figure 1. Structural analogies between 1-ethylKuQuinone and other antitumor molecules.

derivative, having a triethylene glycol side chain, appropriate to enhance solubility in aqueous environment, is presented. Also, a screening of the antitumor activity of a series of KuQs has been performed. No attempts have been made to modify the KuQ core, because the pentacyclic structure is essential in binding and interacting with DNA-TopI complex. Hence, structural modifications were exclusively made in the side chain of KuQs and such alterations lead to substantial variations of solubility, hydrophobic character, geometry, and spatial arrangement of the compound.

RESULTS AND DISCUSSION

Synthesis. The synthetic procedure of KuQ compounds is now well established and it easily occurs through a one-pot process;[11,13b] this unusual reaction takes place in the classical S_N2 conditions and entails the dimerization-condensation of two molecules of 2-hydroxy-1,4-naphthoquinone with an alkyl bromide, to form the central five-membered ring with the loss of a carbon atom. Catalytic amount of ferrocene is required, in order to disfavor the otherwise prevalent S_N2 reaction, thus promoting KuQ formation.[11] The outcome of the process appears to be strictly dependent from several parameters, such as the nature of the solvent, the alkyl halide, the alkyl chain length, as well as the presence of other functional groups. The essential role of DMSO, which is probably involved in the reaction pathway, and the use of bromides as alkyl derivatives source have been already discussed.[11]

In the present article, different KuQuinone derivatives, suitable for biomedical applications, have been prepared with the purpose to optimize the corresponding antitumor activity and to improve their solubility in aqueous media, in order to study their equilibria in solution (Scheme 1 and Table 1). The scope of obtaining a significant variation in the side chain of KuQuinones was achieved through different functional groups directly bound at the alkyl bromide reagent.

In analogy with CPT,[20] the synthesis of water-soluble KuQuinone derivatives was considered, hence in addition to KuQuinones **1**–**6**, the triethylenglycole side chain (TEGMe)[21,22] was introduced via esterification of the starting 6-bromohexanoic acid. Such modification led to a remarkable improvement of the solubility of the corresponding derivative in several conventional organic solvents, but KuQ-$(CH_2)_3CO_2$TEGMe (**7**, hereafter KuQTEGMe) was still poorly soluble in aqueous media. Nonetheless, the improved solubility in the other solvents allowed the study of equilibria in solution with UV–vis and ^{1}H NMR techniques.

Equilibria in Solution: Spectroscopic Study. The pentacyclic and fully conjugated structure of KuQuinones is a crucial feature for their application as dye sensitizers in photoelectrochemical devices,[13] being responsible for their intense and broad absorption in the visible region of the spectrum. However, changing solvent properties, significant variations affecting molar extinction coefficients and spectrum shape were observed (Figure 2).

Considering the structural features of KuQuinones, the intramolecular hydrogen bond between enol oxygen and the vicinal carbonyl oxygen (which was confirmed by X-ray)[11] has a fundamental role. Since KuQuinones contains two naphthoquinone units, keto–enol tautomerization could be the cause of such spectral variations. Specifically, four different species are expected (Scheme 2): the enol form, stabilized by the presence of intramolecular hydrogen bond; the enolate form, in which the negative charge is delocalized over the two quinoid units; the external enol in which intramolecular hydrogen bond is not practicable; and the diquinoid species, where there is no conjugation across the five rings because of the formation of a sp^3 carbon.

In such scenario, solvent properties exert a fundamental role, determining the prevalence of one species in solution and influencing the spectral behavior. Keto–enol tautomerization of diketones has been previously investigated and it is established that keto/enol ratio is generally dependent on the solvent polarity.[23] To note, in apolar media enol stabilization due to intramolecular hydrogen bond is more pronounced, since the solvent cannot compete in hydrogen bond formation. As a consequence, at large the amount of enol form is much higher in apolar solvents than in polar ones. Conversely the diquinoid form is usually prevalent in polar solvents because of the favorable hydrogen bond interactions.[24]

Scheme 1. One-Pot Synthesis of KuQs 1-7 Using Appropriate Alkyl Bromides

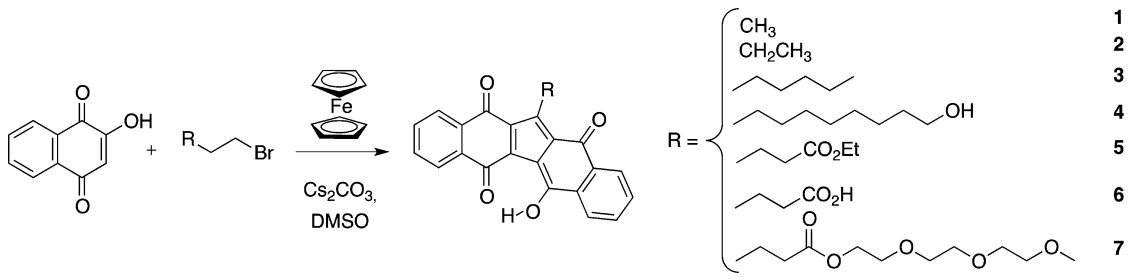

DOI: 10.1021/acs.joc.7b01602
J. Org. Chem. XXXX, XXX, XXX–XXX

Table 1. Reaction Conditions for KuQ Synthesis[a]

	Br-CH_2CH_2-R	KuQ	yield (%)[b]	ref
1	Br-propyl	KuQ**CH_3**	6	11
2	Br-butyl	KuQ**CH_2CH_3**	15	11
3	Br-octyl	KuQ**$(CH_2)_5CH_3$**	6	11
4	Br-$(CH_2)_{11}$OH	KuQ**$(CH_2)_9$OH**	7,5	11
5 (**6**)[c]	Br-$(CH_2)_5CO_2$Et	KuQ**$(CH_2)_3CO_2$Et**	14	13b
7	Br-$(CH_2)_5CO_2$TEGMe	KuQ**$(CH_2)_3CO_2$TEGMe**	9	

[a]2-Hydroxy-1,4-naphthoquinone 0.26 M; alkyl bromide 0.54 M; K_2CO_3 0.36 M; ferrocene 1.5×10^{-2} M; time 41 h, temperature 114 °C. [b]After purification by column chromatography and reiterated crystallizations. [c]Compound **6** obtained through hydrolysis of compound **5** in quantitative yield.

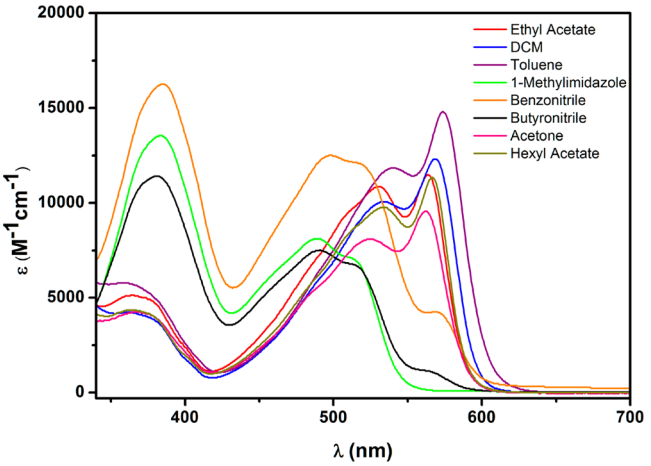

Figure 2. 1-EthylKuQuinone absorption spectra in different solvents (concentration range 2−6 μM).

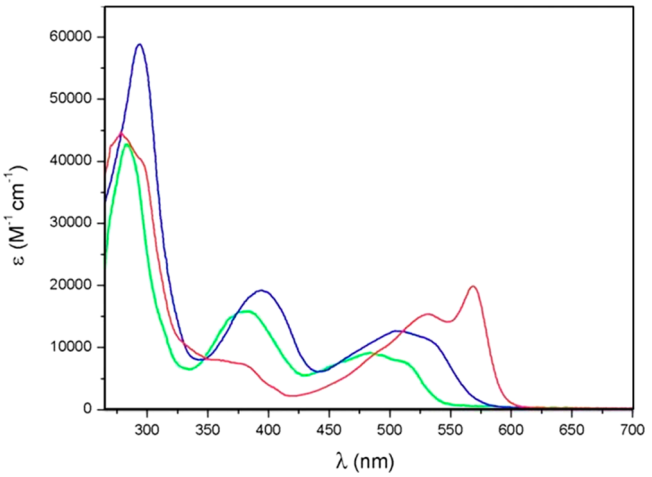

Figure 3. Absorption specta of 1-(3-MeTEGcarbonylpropyl)-KuQuinone $5.6 \cdot 10^{-6}$ M in $CHCl_3$ (red line), MeOH (blue line), and DMSO (green line).

Scheme 2. Possible Keto−Enol Tautomerism in KuQuinones

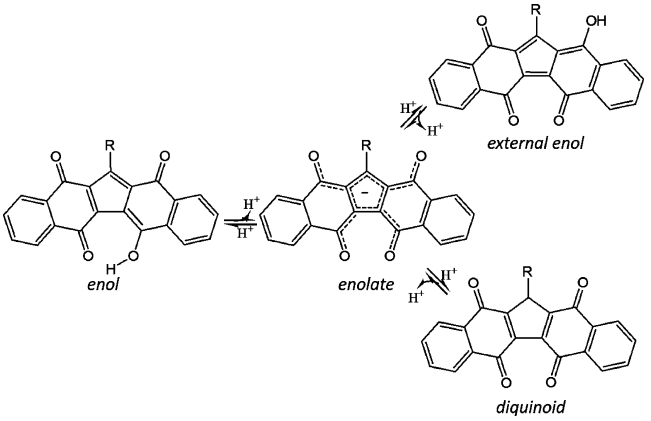

For this reason, to better clarify KuQuinones equilibria in solution, spectroscopic experiments have been performed in three solvents, differing in polarity and ability to participate in hydrogen bond formation (Figure 3). In particular, chloroform, dimethyl sulfoxide, and methanol have been used being, respectively, slightly polar, aprotic polar, and protic polar solvents. Such study resulted an appropriate tool to understand the nature of the prevalent KuQs species in biological media that are responsible for their antitumor activity.

Herein, KuQTEGMe has been used as model compound because, with respect to other KuQuinone derivatives, it showed an improved solubility in many conventional organic solvents, thanks to the triethylenglycole side chain. Nevertheless, differences in side chain do not influence absorption spectrum of KuQuinones as well as their equilibria in solution.

Regarding KuQTEGMe absorption spectra in different solvent, significant alterations in the shape have been observed in the region above 350 nm: in chloroform, the UV−vis spectrum is characterized by two bands between 450 and 600 nm, with a relative maximum of absorption approximately at 530 nm and the absolute maximum around 570 nm (red line). The figure recorded in chloroform can be reasonably assigned to the enol form of the KuQuinone derivative. Experimental proof can be found in the ^{1}H NMR recorded in the same solvent (Figure S3 in SI) in which the enol proton is visible at 18 ppm. The intramolecular hydrogen bond is evident from the characteristic chemical shift of this signal, which is strongly deshielded.[12,25] This allows excluding the presence of the external enol form of the molecule in chloroform, where intramolecular hydrogen bond would not be possible, and the corresponding signal would be expected at higher fields.

Considering the exclusive presence of the enol form of KuQuinone in $CHCl_3$, the aid of an excess of a basic component reasonably imply deprotonation of the enol group, generating the enolate species. As a result, a strong spectral variation has been obtained (Figure S8 in SI). Noticeably, the obtained spectral profile, that is diagnostic of the enolate form, perfectly matches with the shape of the spectrum in DMSO. Referring to the spectra in DMSO, the maximum of absorption is shifted between 350 and 400 nm, while bands between 450 and 550 nm are inverted in relative intensities with respect to those in chloroform and shifted at

DOI: 10.1021/acs.joc.7b01602
J. Org. Chem. XXXX, XXX, XXX−XXX

lower wavelengths. Moreover, also ^{1}H NMR spectrum recorded in DMSO-d_6 (Figure 4) allows the enolate form of

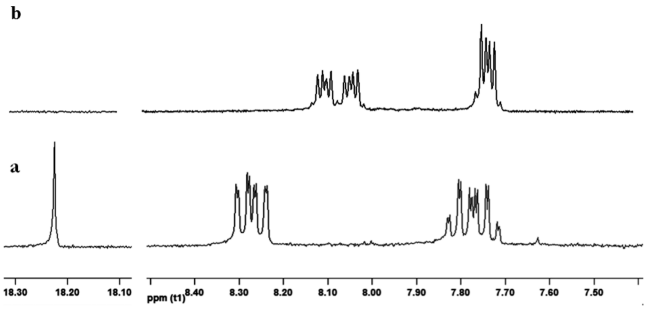

Figure 4. Comparison between ^{1}H NMR spectra of KuQTEGMe in (a) $CDCl_3$, (b) DMSO-d_6.

KuQTEGMe identification: i.e., the absence of the enol proton signal and the differences in the corresponding aromatic region can be assigned to the negatively charged species. The presence of the enolate species is probably due to water traces dissolved in the solvent and also to its higher basicity in DMSO than in low-polar solvent.

As to KuQTEGMe in MeOH, the shape of the absorption spectrum was halfway to those in DMSO and in $CHCl_3$. It seems plausible that in MeOH the two species (enol and enolate) can coexist in equilibrium, while they are well distinguished in the other two solvents.

To further comprehend such behavior, absorption spectra have been recorded with different concentration of KuQTEGMe. Concerning $CHCl_3$ and DMSO (Figures S9−S10 in SI), no modifications were detected, while strong differences appeared in MeOH (Figure S11 in SI). Specifically, in MeOH, when KuQTEGMe concentration is lower than $1.0\cdot10^{-5}$ M, the prevalent species is the enolate, while at higher concentration aggregation phenomena may occur, causing the broadening of the spectrum. Namely, aggregates formation can be favored by the planar, pentacyclic, and fully conjugated structure of KuQuinone, where π-stacking and intermolecular hydrogen bonds may easily take place.

In the presence of a base, i.e., water, a continuing spectral modification appears, due to the progressive deprotonation of the enol group, which leads to the negatively charged system formation (Figure 5). In this latter case, the charge is delocalized across the KuQuinone core and the charge repulsion inhibits the aggregation, also at high concentration.

To validate the assumptions, ^{1}H NMR spectra in CD_3OD have been performed at different concentrations. In methanol, the absence of the enol proton signal, due to the −OH exchange with deuterium in the solvent, hampers the detection of the enolate form. The most important difference between the spectra involves the aromatic region (Figure 6). In particular, at low concentration, the spectrum is well resolved and also the multiplicity of the signals is well-defined. At higher concentrations, loss of the resolution of the spectrum is observed, confirming the hypothesis that in methanol, aggregation phenomena occur.

To summarize, experimental data suggest that in the solvents used, KuQuinones undergo acid−base equilibrium on the enol group (Scheme 3). Indeed, the observed spectral variations are easily attributed to the acid−base behavior of the enol; while aggregation phenomena are more plausible in concentrated solutions.

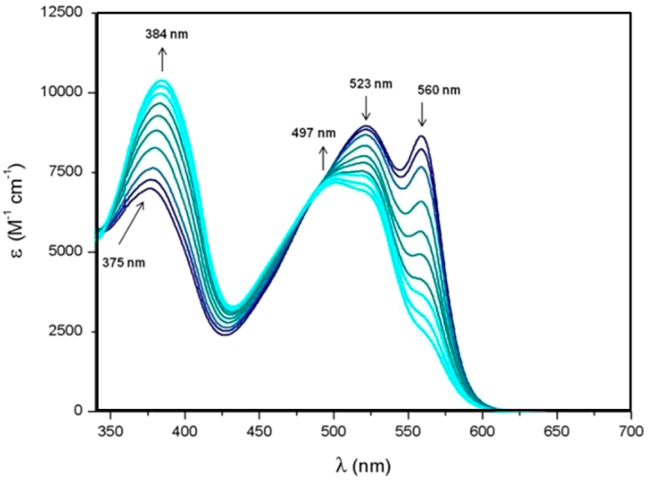

Figure 5. Spectral variation by water titration of KuQTEGMe 10^{-4} M in MeOH (from dark blue to light blue).

Further, no spectroscopic evidence has been achieved to confirm the existence of the diquinoid species or external enol species in solution. For this reason, the pK_a value of KuQTEGMe has been calculated from absorption spectra by dissolving KuQTEGMe in MeOH and diluting it in aqueous solution at different pHs (more details are given in SI). At pH values lower than 5.6 the obtained absorption spectra are typical of the enol form of the KuQuinone, while at higher pHs a strong variation of the spectrum appears, indicating the presence of the deprotonated species. The variation of the absorbance at 585 nm from pH describes a sigmoidal curve used for calculating a pK_a = 4.7 ± 0.1. Such a low pK_a may explain why in MeOH and DMSO water traces may capture the acid enol proton.

Equilibria in Solution: DFT Calculations. To substantiate experimental data, DFT calculations have been performed, using hybrid functional B3LYPor PBE0 and 6-31G+dp basis set for geometry optimization and B3LYP 6-311G++dp basis set both in vacuum and using the PCM (polarized continuum model) with water as solvent, in single point energy calculation. In order to simplify the model 1-methylKuQuinone was utilized (Figure S16 in SI). Results point out the higher stability of the enol form with respect to the diquinoid and the external enol species. Obtained energy values for all the species are reported in Table 2. Same calculations for the enolate species are not directly comparable with the other neutral species because of the presence of the charge.

Experimental pK_a values have been also compared with theoretical ones, calculated using Gaussian 09[26] and Jaguar[27] programs.

With Gaussian 09, pK_a calculations with the aid of two water molecules have been performed. In fact, previous works have demonstrated that pK_a determination performed using non-solvated species offered unsatisfactory results. Accordingly, two water molecules should be preferably added to both the neutral and anionic species (Figure 7).[28]

Hence, the pK_a determination of a generic acid HA can be performed by taking into account the following proton-transfer reaction:

$$HA(H_2O)_2 + OH^-(H_2O)_2 \rightarrow A^-(H_2O)_2 + H_2O(H_2O)_2 \quad (1)$$

that gives eq 1 for pK_a calculation at 298.15 K:

DOI: 10.1021/acs.joc.7b01602
J. Org. Chem. XXXX, XXX, XXX−XXX

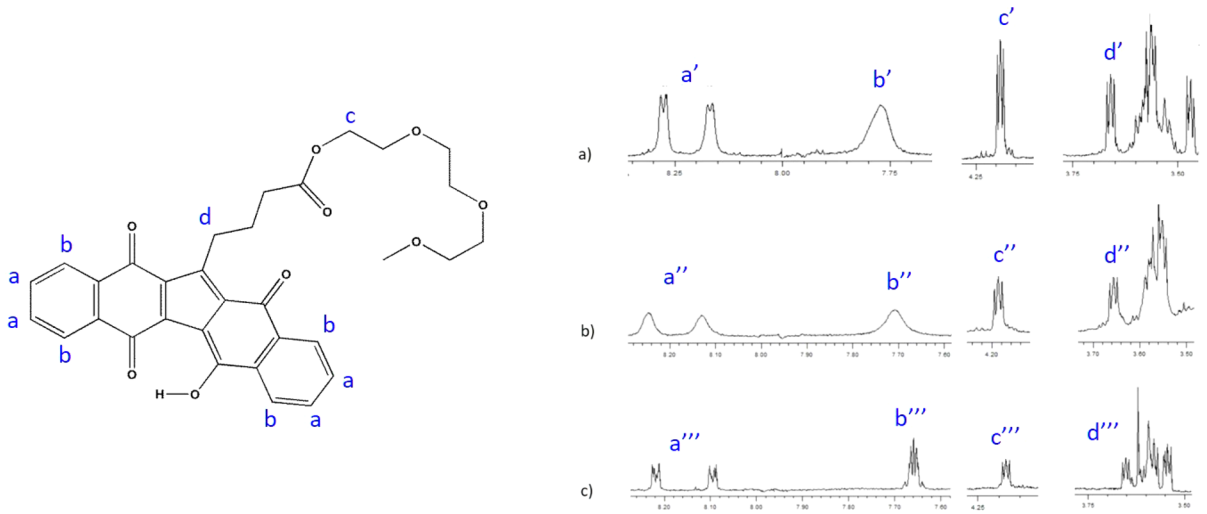

Figure 6. ^{1}H NMR spectra in MeOD: (a) $1.0\cdot10^{-5}$ M; (b) $5.0\cdot10^{-6}$ M; (c) $1.0\cdot10^{-6}$ M.

Scheme 3. Acid−Base Equilibrium of KuQuinone

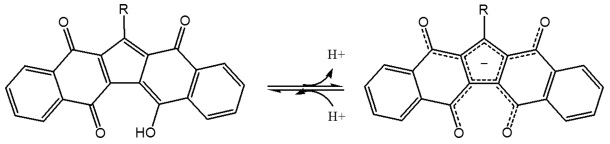

Table 2. Calculated Energy of 1-MethylKuQuinone in Vacuum and in Water (PCM)

ΔE (kcal·mol^{-1})	enol	external enol	diquinoid
vacuum	0	16.0	20.0
water	0	11.0	10.5

$$pK_a = (\Delta G_{solv}/2.3RT) - 15.74 \quad (2)$$

where:

- ΔG_{solv} is the solvation free energy,[29] theoretically calculated using integral equations formalism polarized continuum model (IEF-PCM method) B3LYP 6-311G++(d,p).
- 15.74 is the pK_a value for pure water.

Such calculations were applied to estimate KuQuinone pK_a value. In order to simplify the model, 1-methylKuQuinone is still used as reference molecule. Water contribution in the model can be observed in the stabilization of the negatively charged molecule through the formation of hydrogen bonds, while in the enol species the contribution is expected to be low, because of the preferred intramolecular hydrogen bond (Figure 7).

Same calculations were performed for 2-hydroxy-1,4-naphtoquinone (NQ). In fact, since these systems can be constructed in several models, it is preferable to compare, in the same settings, calculated pK_avalue with those of a simpler reference molecule. For this reason, NQ with two water molecules has been used as reference.

The pK_avalue for 1-methylKuQuinone (KuQMe) can be corrected as follows:

$$pK_{a\,KuQMe}(\text{corrected}) = pK_{a\,KuQMe}(\text{calc}) - [pK_{a\,NQ}(\text{calc}) - pK_{a\,NQ}(\text{exp})]$$

$$pK_{a\,KuQMe}(\text{corrected}) = 1.89 - [1.58 - 4.50] = 4.81$$

Thus, pK_a = 4.81 has been calculated using Gaussian 09, which is well in line with the experimental one (4.7 ± 0.1).

Lower pK_a values for both molecules have been directly calculated using Jaguar software:

$$pK_{a\,KuQMe}(\text{calc}) = 4.2$$

$$pK_{a\,NQ}(\text{calc}) = 3.1$$

Equilibria in Solution: Gas-Phase Analyses. In order to understand acid−base equilibrium of KuQs inside the cell, MS-

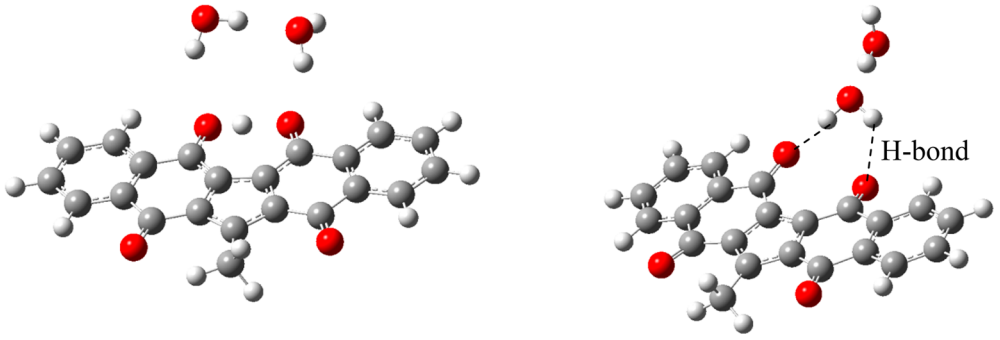

Figure 7. Optimized geometries (B3LYP 6-31G+dp basis set) for 1-methylKuQuinone with two water molecules (enol form on the left and enolate species on the right).[26]

DOI: 10.1021/acs.joc.7b01602
J. Org. Chem. XXXX, XXX, XXX−XXX

ESI gas-phase analyses have been performed, considering that gas-phase could be a model of the lipophilic region of the cell.

In this experiment, proton affinities, defined as the negative of the enthalpy change ($-\Delta H$) for the reaction[30]

$$A^- + H^+ \rightarrow HA$$

are available by measuring the equilibrium constant for a reverse proton-transfer reaction to a second base, as a function of the temperature.[31,32]

Also in the MS-ESI gas phase analysis, 2-hydroxy-1,4-naphtoquinone has been used as the reference compound. Specifically, the anions $KuQMe^-$ and NQ^- have been readily formed upon electrospray ionization of a CH_2Cl_2-MeOH (1:4) solution containing equimolar amounts (10^{-3} M) of both KuQMe and NQ. The experiment involves the competitive fragmentation of proton-bound dimers composed by a proton and the two ionized compounds under examination (Scheme 4).

Scheme 4. Competitive Fragmentation of Proton-bound Dimers of Ionized KuQ and NQ in the Presence of a Proton

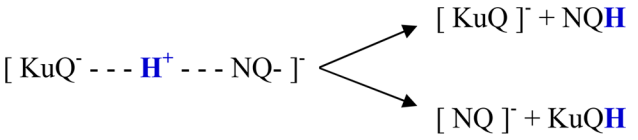

Collision induced dissociation of $[KuQ\text{---}\mathbf{H}\text{---}NQ]^-$ likely results in the observation of both anions. If the relative abundance of the peak pertaining to KuQ^- is higher than that of NQ^-, as in the experiment shown in Figure 8, it retains a lower proton affinity with respect to NQ^-, and therefore a higher gas-phase acidity.

In order to establish a more precise comparison of proton affinities of KuQ and NQ anions, gas-phase reactivity of both KuQMe and NQ has been compared with that of compounds with known anion proton affinity, namely two benzoic acid derivatives.[33]

The experiments unambiguously indicated the proton affinity order reported in Scheme 5, assessing the higher acidity in gas-phase of KuQuinone with respect to the structurally related compound NQ.

DFT calculations also confirmed these data. In particular, following geometry optimization of anionic and neutral species of both NQ and KuQ (using B3LYP 6-31G+dp basis set), zero point energies have been calculated using B3LYP 6-311G++dp level of theory. The energy difference (ΔE) between the anionic and the neutral species of NQ in the vacuum (thus simulating the gas-phase analysis) was almost 0.5 kcal/mol higher than that of KuQ. Such result indicates a lower stability of the anionic NQ species in the vacuum and consequently a higher proton affinity, confirming the lower acidity of NQ than KuQ in the gas-phase analysis (Table 3).

To conclude, it has been observed that acidity trends for KuQuinones and 2-hydroxy-1,4-naphtoquinone in the gas phase and aqueous solvent (both experimentally and theoretically calculated) are divergent: in particular as expected aqueous solvation has a key role in determining stability and acidity of the studied molecules. Specifically, NQ anion is smaller than KuQ anion and in NQ^- the negative charge is delocalized over two rings instead of five. For these reasons, the energy gain due to solvation in water should be higher with respect to KuQ^-. Hence, solvation implies higher stability of NQ^- than KuQ^- and lower proton affinity in aqueous solution. Conversely, no solvation effect can be expected in the gas-phase where the negative charge is more delocalized in KuQ^- than in NQ^-. Such extended delocalization implies higher stability of KuQ^- and consequently higher acidity than NQ in the gas phase.

Cytotoxic Activity Against Human Cell Lines. Inhibition of growth in SW480 and SKOV3 cell lines by the new KuQs was evaluated by the colorimetric MTT assay, which provides a quantitative estimation of the number of viable and metabolically active cells in a culture. As reported in Table 4, all the compounds show an efficient antiproliferative activity, in agreement with previous results.

Referring to SW480, all the IC_{50} values are lower than, or equal to 21 μM, suggesting that this experimental setting is more sensitive than the previous one (Figure S17). Results indicate that compounds **2**, **3**, **5**, and **7** have an IC_{50} value lower than 10 μM. This result is likely correlated to the presence of

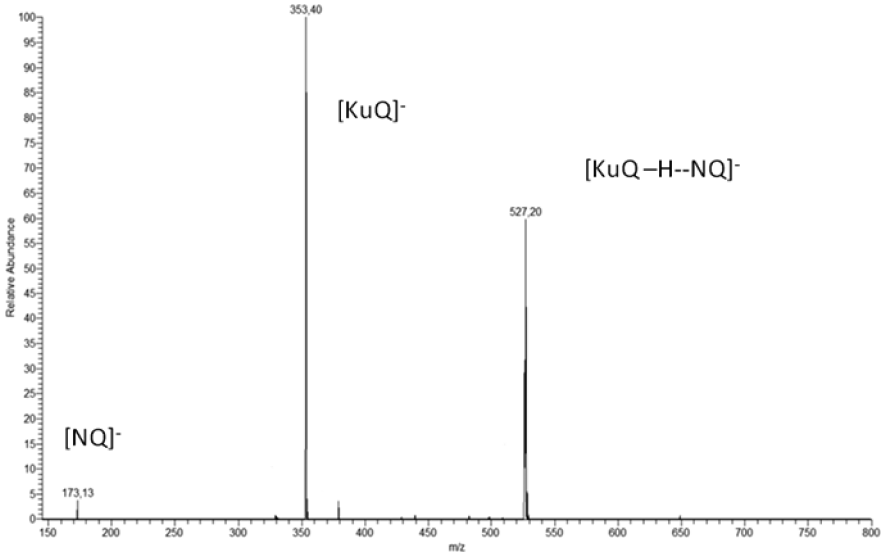

Figure 8. Obtained MS-ESI spectra for gas-phase proton affinity analysis.

DOI: 10.1021/acs.joc.7b01602
J. Org. Chem. XXXX, XXX, XXX−XXX

Scheme 5. Proton Affinity Order for the Analyzed Molecules

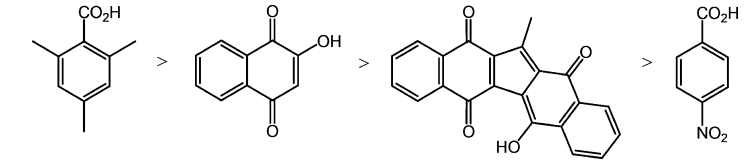

Table 3. Calculated Energy Difference (ΔE) between Anionic and Neutral Species in the Vacuum

	ΔE (kcal·mol^{-1})
KuQMe	327.031
NQ	327.517

Table 4. Growth Inhibition Concentrations in SW480 and SKOV3 Cell Lines and in Healthy Human Fibroblasts (HF) by KuQanalogues[a]

	IC_{50}(μM) SW480	IC_{50}(μM) SKOV3	IC_{50}(μM)	SI[b] SW480	SI[b] SKOV3	log$P$[c]
1	20.4 ± 3	27.8 ± 3	24 ± 3	1.2	0.86	0.63
2	8.5 ± 3	4.8 ± 2	37 ± 5	4.4	7.7	1.05
3	9.6 ± 5	5.5 ± 4	245 ± 8	25.5	44.5	2.72
4	21.5 ± 2	24.8 ± 3	>400	>20	>20	2.77
5	7.8 ± 2	25.7 ± 3	380 ± 7	48.7	14.8	1.08
6	19.3 ± 2	52.2 ± 6	92.5 ± 6	4.8	1.8	0.48
7	1.5 ± 2	35 ± 6	72.3 ± 6	48.2	2.1	0.28
CDDP	4.2 ± 1	10.4 ± 2	25 ± 4	5.9	2.4	

[a]All the compounds were incubated with cells for 72 h and tested by MTT assay. Results were determined from the dose−response curves and are expressed as average of three independent experiment ± SD. [b]Calculated values: IC_{50} healthy cells/IC_{50} cancer cells. [c]Software calculations.

apolar or low polar side chains, but further studies are still necessary to confirm such hypothesis. Interestingly, compound **5** has an IC_{50} value only double than that of CDDP (≈ 8 and ≈4 μM, respectively) while compound **7** is four times more effective than the reference molecule, as shown in Figure 9.

TEG modification may help compound **7** cellular uptake, changing the interactions with the lipophilic and hydrophilic parts of the cells, thus allowing the molecule to easily cross the membrane. These results suggest that the modification in alkyl side chain significantly affects the antitumor activity of KuQs on SW480 cellular line. Indeed, IC_{50} ranges among a very low

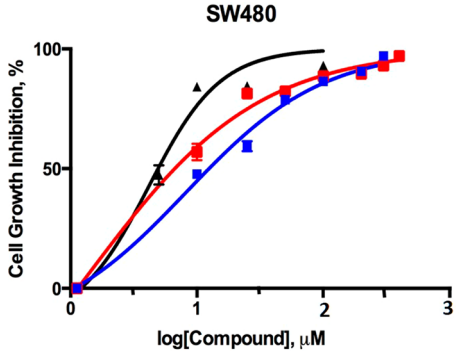

Figure 9. Antiproliferative activity of **5**(blue line), **7** (red line), and CDDP (black line) against SW480 cell line after 72 h. Average of three independent experiments ± SD.

value (as for compound **7** ≈ 1,5 μM) to high ones (≈ 21 μM for compound **4**). This evidence supports the hypothesis that the nature of the side chain strongly affects the cellular uptake, rather than trigger the mechanism of drug resistance. A less clear trend has been observed with SKOV3 cells: here a wide variation in IC_{50} values has been observed. They fluctuate from ≈5 μM (that is a very promising value, being two times lower than that of CDDP) up to ≈52 μM. Compounds **2** and **3**, having hydrophobic chains, are the most efficient ones, and the dose that caused the 50% of growth inhibition is lower than that of CDDP (Figure 10). Compounds **1**, **4**, and **5** have similar

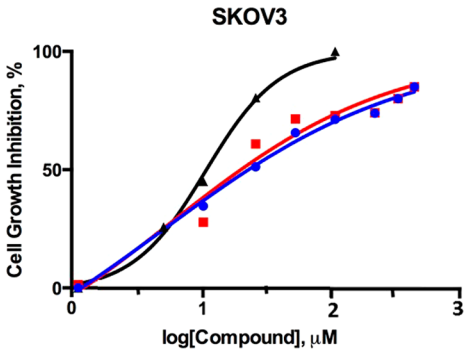

Figure 10. Antiproliferative activity of **2** (blue line), **3** (red line), and CDDP (black line) against SKOV3 cell line after 72 h. Average of three independent experiments ± SD.

IC_{50} values ≈26 μM while compound **7** has an IC_{50} value close to 35 μM, suggesting a cellular membrane composition for SKOV3 very different from that of SW480.

To note, compounds **2** and **3** show a toxic dose only 2 orders of magnitude higher than CPT (the IC_{50} values for CPT on SKOV3 is in the nanomolar range),[34] but their cytotoxic activity toward healthy HF confirms the appealing of the KuQ library as antitumor agents (Table 4 and Figure S19). In fact, results highlight that compounds **3**, **4**, and **5** have the highest IC_{50} values against HF, larger than 200 μM, and compounds **6** and **7** show an IC_{50} lower than 100 μM (≈ 93 and ≈72 μM, respectively). This is a very promising result, in particular considering that CPT usually shows high toxicity on healthy cells. Moreover, further modifications on the side chain of KuQs may still improve these values.

Overall, the KuQ analogues tested, with the exception of **1** in SW480 and **1**, **6**, and **7** in SKOV3, showed very high SI values. In fact, compounds **3** and **5** demonstrate an antitumor activity toward SW480 slightly higher than that of CDDP, but they have significantly lower toxicity against human fibroblasts. Among the tested KuQ derivatives, the most efficient one was compound **3**, i.e., 1-hexylKuQuinone, that showed the best result in terms of IC_{50} for both cancer cell lines. In detail, compound **3** exhibits promising antiproliferative activity and a selectivity index greater than 44 and 25 for SW480 and SKOV3,

DOI: 10.1021/acs.joc.7b01602
J. Org. Chem. XXXX, XXX, XXX−XXX

respectively. To note, cytotoxicity for human fibroblast is higher than 200 μM (Figure 11).

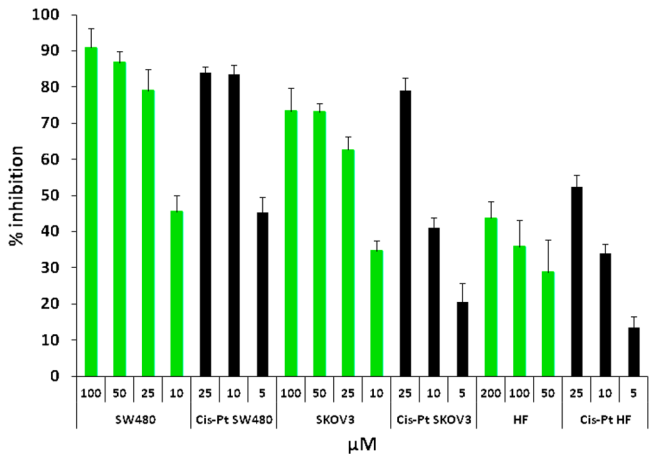

Figure 11. Comparison between KuQHex (**3**, green bars) and Cisplatin (CDDP, black bars) antiproliferative and cytotoxic activities. Average of three independent experiments ± SD.

In order to correlate physical and chemical properties with the cytotoxic activities, we used the log*P* values for the KuQ compounds, as obtained by software calculations (see Experimental Section for details). This parameter relates to the lipophilicity of a molecule and represents a key parameter to describe the ability to cross biological membranes and therefore the pharmacokinetic processes. It is usually defined as the partition of the compound between aqueous and nonaqueous phases, namely between water and 1-octanol ($\log P_{o/w}$). In addition it is possible to estimate the log*P* through software calculations and/or appropriate chromatographic methods.[35−37] Introduction of different alkyl chains and/or functional groups allowed to obtain significant variations of the log*P* value (Table 4), as well as a remarkable difference in geometry. The lowest value of log*P* has been shown for the KuQ derivative containing the triethylene glycol mono methyl ether chain (**7**), while the most hydrophobic compound is the one with a γ-hydroxynonyl chain (**4**). A simple correlation between log*P* calculated values and the corresponding antiproliferative activities is not observable, probably because several factors are involved in the structure−activity relationships of KuQs compounds. In fact, besides the compounds diffusion across cellular membranes, which is generally well described by log*P* parameter, the ability to react with target biological macromolecules should also be considered (polarizability, molecular volume, etc.).[38]

All the reported results suggest to investigate KuQs derivatives further as antitumor drugs on the basis of the toxic effect on treated tumor cells. However, the toxic power of each molecule is strictly associated with the cellular line. Compound **7** is the most promising drug against SW480, even if its IC_{50} in human fibroblast is not negligible. Instead, compounds **3** and **5** show IC_{50} values double than that of CDDP and very promising behavior on healthy cells. Referring to SKOV3, compounds **2** and **3** have the highest toxicity, but only compound **3** is nontoxic toward human healthy cells. As wide-ranging antitumor agent with high activity toward different tumor cells and negligible effect on healthy ones, molecule **3** should be the choice.

CONCLUSIONS

In this article, a detailed investigation of KuQuinones behavior in solution has been performed in order to recognize their role as antitumor agent.

In particular, UV−vis and ^{1}H NMR studies have been carried out in different organic solvents in order to understand the nature of the species in solution. To date, experimental evidence suggests that the enol and the enolate forms of KuQuinones, caused by the acid−base reaction at the enolic group, are the only species in solution. Same behavior can be expected in biological environment. Theoretical calculations wholly support the mentioned experimental evidence, demonstrating that other possible tautomers (i.e., the external enol and the diquinoid species) are energetically unfavored.

Such acid−base equilibrium in KuQuinones is likely the driving force that is responsible of the KuQs antitumor activity, allowing it to strongly interact with the DNA-TopI complex.

In this context, the activity of diverse KuQs (differing in side chain length and functional groups) has been tested to further improve their performances as antitumor agents. Results highlighted that KuQs are highly active toward the analyzed cell lines. In particular, for SW480 line, compound **7** shows the highest efficiency while compounds **2**, **3**, and **5** are toxic at a dose double than that of CDDP. Similar results were obtained also for SKOV3, with compounds **2** and **3** being the most efficient ones. Calculation of SI helps the identification of the most promising compound and in this context molecule **3** resulted almost nontoxic for healthy cell, indicating high specific activity toward tumor cell.

EXPERIMENTAL SECTION

Materials and Methods. *Instrumentation.* The purity of the synthesized compound was checked by HPLC analysis using a UV−vis detector, equipped with an Ascentis Express F5 150 × 4.6 mm column and CH_3CN/H_2O 3:2 as eluent; all the compounds were ≥99% pure. High-resolution mass and NMR spectrometry were used to characterize and confirm the structure of all the synthesized compounds; in particular, NMR spectra were recorded in saturated $CDCl_3$ solutions with a spectrometer operating at 300.13 MHz for ^{1}H and at 75.43 MHz for ^{13}C. The NMR peak assignments were confirmed by DQF-COSY at 600.013 MHz. GC/MS were performed using a Supleco SLB-5MS column. DFT calculations (geometry optimization and single point energies) have been performed with Gaussian 09 rev. A02.[26] Theoretical pK_a determination has been performed using Gaussian 09 and Jaguar. log*P* calculations were performed using SPARTAN'10 Wave function, Inc., Irvine, CA, at B3LYP level with 6-31 G* basis set.

Synthesis. The optimized synthetic procedure for KuQs**1**−**6** was recently reported.[11,13b] Reagents were purchased and used without further purification. Spectrophotometric grade DMSO was kept over anhydrous K_2CO_3 overnight prior to use. Glassware was dried under N_2.

Synthesis of Methoxy Triethylene Glycolyl 6-Bromohexanoate. 6-Bromohexanoic acid (4.9 g, 25 mmol) was dissolved in 25 mL of triethylene glycol monomethyl ether and 150 μL of 37% HCl have been added. The reaction mixture was kept under stirring at 40 °C for 3 days. It was then diluted with 100 mL of dichloromethane and extracted with small portions of water and brine (6 × 30 mL). Organic phase was dried over Na_2SO_4, filtered, and the solvent was evaporated under reduced pressure. Afterward, it was dried at the vacuum pump to eliminate residual water. A pale yellow liquid was obtained (8.5 g; yield >99%) and it was characterized by ^{1}H NMR analysis. ^{1}H NMR ($CDCl_3$, 300 MHz): δ 4.26−4.22 (m, 2H), δ 3.72−3.64 (m, 8H), δ 3.57−3.54 (m, 2H), δ 3.44−3.41 (t, J = 6.30 Hz, 2H), 3.39 (s, 3H), δ 2.39−2.34 (t, J = 7.34, 2H), δ 1.91−1.86 (m, 2H), δ 1.70−1.64 (m, 2H), δ 1.52−1.46 (m, 2H). ^{13}C NMR ($CDCl_3$, 300 MHz): δ 172.9 (C

DOI: 10.1021/acs.joc.7b01602
J. Org. Chem. XXXX, XXX, XXX−XXX

= O), 71.5, 70.2, 70.10, 68.7, 63.0, 58.6 (MeTEG carbons), 33.5, 33.0, 31.9, 27.2, 23.6 (aliphatic carbons). GC/MS pure 99% m/z: 220.85 (100%), 222.81 (98%) $[M\text{-}C_5H_{11}O_3]^+$. Anal. Calcd for $C_{13}H_{25}BrO_5$: C, 45.76; H, 7.38. Found: C, 45.82; H, 7.76.

Synthesis of 1-(3-MeTEGcarbonylpropyl)KuQuinone (KuQTEGMe) (7). The reaction was carried out using methoxy triethylene glycolyl 6-bromohexanoate as alkyl bromide and according to the general procedure.[11] 12 mmol of the alkyl bromide were added to 2.5 g (8 mmol) of anhydrous Cs_2CO_3, 1 g (5.75 mmol) of 2-hydroxy-1,4-naphthoquinone, and 62 mg (0.33 mmol) of sublimated ferrocene in 22 mL of DMSO. The brown powder obtained was purified by plug chromatography (SiO_2, CH_2Cl_2 and MeOH 1% as eluent). Isolated product was repeatedly crystallized from dichloromethane-hexane and washed with pentane. A purple powder was obtained (146 mg, yield: 9%) and was characterized. ^{1}H NMR ($CDCl_3$, 300 MHz): δ 18.12 (s, 1H), δ 8.22−8.15 (m, 4H), δ 7.76−7.65 (m, 4H), δ 4.25−4.22 (t, J = 5.04 Hz, 2H), δ 3.71−3.64 (t, J = 5.04 Hz, 2H), δ 3.59−3.52 (m, 6H), δ 3.48−−3.37 (m, 4H), δ 3.34 (s, 3H), δ 2.53−2.51 (t, J = 7.80 Hz, 2H), δ 2.10−2.05 (m, 2H). ^{13}C NMR: δ 180.5, 177.7, and 173.1 (C=O); 148.8, 135.3, 134.7, 132.7, 132.3, 131.5, 127.4, 126.8, and 125.2 (aromatic carbons); 71.5, 70.2, 68.8, 63.0, 58.6, 33.7, 26.0, and 24.0 (aliphatic carbons). HRMS (ESI-) m/z: $[M-H]^-$calcd. for $C_{32}H_{29}O_9$ 557.1817; found 557.1839. Anal. Calcd for $C_{32}H_{30}O_9 \cdot H_2O$: C, 66.70; H, 5.60. Found: C, 67.38; H, 5.70. mp 77−80 °C.

Experimental pK_a Determination. p$K_a$value of KuQTEGMe has been determined from absorption spectra as a function of pH. To this aim aqueous solutions at different pH have been prepared using HCl and NaOH. pK_a value was determined using the inflection point of the obtained curve.

pK_a for 2-Hydroxy-1,4-naphtoquinone (NQ). NQ (5.4 mg) was dissolved in 5 mL of spectrophotometric grade methanol ([NQ] = $6.2\cdot10^{-3}$ M). Thirty microliters of this solution was added in a cuvette containing 1.8 mL of water (at the different pH values). Concentration of NQ in the cuvette was $1.0\cdot10^{-4}$ M. UV−vis absorption spectrum of the resulting solution was recorded and, in particular, the absorbance of the band centered at 453 nm was followed in order to calculate the pK_a value for NQ.

pK_a for KuQTEGMe. KuQTEGMe (1.2 mg) was dissolved in 5 mL of spectrophotometric grade MeOH ([KuQTEGMe] = $4.3\cdot10^{-4}$ M). Ninety microliters of this solution was added in a cuvette containing 1.8 mL of water (at the different pH values). Concentration of NQ in the cuvette was $2.0\cdot10^{-5}$ M. UV−vis absorption spectrum of the resulting solution was recorded and the behavior of the band centered at 585 nm was followed for pK_a determination.

Theoretical pK_a Determination. Theoretical pK_a determinations were performed using Gaussian 09 (following previously reported literature procedures)[26,28] and Jaguar[27] programs.

Gas-Phase Analyses. ESI mass spectra were obtained in negative-ion mode, by introducing a 1:1 mixture of two selected compounds dissolved in CH_2Cl_2-MeOH (1:4). Instrumental parameters: capillary voltage −10 V, spray voltage 4.50 kV, capillary temperature of 160 °C, mass scan range was from m/z 100 to 1000 amu, for 30000 ms scan time; N_2 was used as sheath gas. MS/MS mass spectra of hetero proton-bound dimers were performed upon isolation of the selected dimeric species and application of normalized collision energies from 10 to 25% of the instrument maximum. The samples were injected into the spectrometer by a syringe pump at a constant flow rate of 8 mL·min^{-1}.

Cell Lines and Culture. The colon cancer cell line SW480 and the ovarian cancer cell line SKOV3 were obtained from ATCC (Manassas, VA) and maintained in RPMI 1640, supplemented with 10% fetal bovine serum (FBS), penicillin (100 U mL^{-1}), streptomycin (100 μg mL^{-1}), and glutamine (2 mM). Human fibroblast cells were maintained in DMEM, supplemented with 10% fetal bovine serum, penicillin (100 U mL^{-1}), streptomycin (100 μg mL^{-1}), and glutamine (2 mM). The pH of the medium was 7.2 and incubation was performed at 37 °C in a 5% CO_2 atmosphere. Cells were routinely passaged at 70% of confluence using 0.05% trypsin-EDTA (Lonza). The antiproliferative activity of compounds was tested with MTT assay.[39]

MTT Assay. The MTT test was used to study the antiproliferative activity of compounds. In a typical experiment, cells were seeded in triplicate in 96-well, keeping initial density of 5×10^3 for both cancer cells and human fibroblasts. Each compound was dissolved in DMSO, obtaining a stock solution (20 mM) that was diluted in RPMI or DMEM medium, according to cells type, to achieve different final concentrations (10, 50, 100, 200, 300, and 400 μM, respectively). As controls, cells were treated with the same contents of DMSO alone. According to the protocol, cells were exposed to each compound at fixed concentration for 72 h, after that the colorimetric assay was performed. Briefly, cells were filled using a total media volume of 100 μL, containing the selected drug at the aforementioned concentrations, and then 25 μL of 3-(4,5 dimethylthiozol-2-yl)2,5-diphenyltetrazolium bromide solution (MTT) (12 mM) were added to each well. Plates were incubated at 37 °C and 5% CO_2. After 2 h, the MTT medium was removed, the cells were rinsed with PBS, and 100 μL of DMSO was applied. The plates were shaken on a microtiter plate shaker for 20 min to extract and solubilize the MTT violet colored formazane crystals from the cells and form a homogeneous solution. The solution absorbance, proportional to the number of live cells, was measured using a spectrophotometer at 570 nm and converted into % of growth inhibition.[40] Compounds inhibition, that caused the 15% of cells death (IC_{50}), was established fitting data using Prims6 (GraphpadSowftwer Prims6, SanDiego, CA). Each value represents the mean of three independent experiments and data were analyzed using the dose−response curve-stimulation. In the graphs, compounds concentration were expressed as Log of drug amounts by relating with the absorbance of MTT test. Data were normalized to the untreated control, which contained the same quantity of DMSO without drugs, and reported as the value that arouses the corresponding growth inhibition. Because of compounds are poor soluble in water media, even if the predilutions in DMSO, the curves were forced to 100% of cells death to settle the IC_{50} values.

■ ASSOCIATED CONTENT

Supporting Information

The Supporting Information is available free of charge on the ACS Publications website at DOI: 10.1021/acs.joc.7b01602.

NMR spectra of new synthesized compounds (^{1}H, ^{13}C, and DQF-COSY), HRMS analysis, LC-chromatogram, UV−vis spectra of KuQTEGMe in different solvents, pK_a titration, DFT optimized Cartesian coordinates and energies, and antiproliferative activity of different KuQs against SW480 and SKOV3 cell lines (PDF)

■ AUTHOR INFORMATION

Corresponding Author

*E-mail: galloni@scienze.uniroma2.it; Fax: +39 0672594328.

ORCID

Olga Bortolini: 0000-0002-8428-2310

Pierluca Galloni: 0000-0002-0941-1354

Notes

The authors declare no competing financial interest.

■ ACKNOWLEDGMENTS

P.G. thanks University of Rome Tor Vergata "'Ricerca Scientifica d"Ateneo 2015" for financial support to, SMART project". F.S. acknowledges the financial support from the project "Spectroscopic and computational study of intra-molecular LB-HB in highly conjugated polycyclic systems".

■ REFERENCES

(1) See as example: (a) Barnes, T. A.; Amir, E.; Templeton, A. J.; Gomez-Garcia, S.; Navarro, B.; Seruga, B.; Ocana, A. *Cancer Treat. Rev.* **2017**, *56*, 1−7. (b) Redondo-Blanco, S.; Fernández, J.; Gutiérrez-del-

DOI: 10.1021/acs.joc.7b01602
J. Org. Chem. XXXX, XXX, XXX−XXX

Río, I.; Villar, C. J.; Lombó, F. *Front. Pharmacol.* **2017**, *8*, No. 109, DOI: 10.3389/fphar.2017.00109. (c) Tartarone, A.; Giordano, P.; Lerose, R.; Rodriquenz, M. G.; Conca, R.; Aieta, M. *Med. Oncol.* **2017**, *34*, No. 110, DOI: 10.1007/s12032-017-0966-6. (d) Li, Y. J.; Lei, Y. H.; Yao, N.; Wang, C. R.; Hu, N.; Ye, W. C.; Zhang, D. M.; Chen, Z. S. *Chin. J. Cancer* **2017**, *36*, No. 52, DOI: 10.1186/s40880-017-0219-2.

(2) Kapadia, G. J.; Balasubramanian, V.; Tokuda, H.; Konoshima, T.; Takasaki, M.; Koyama, J.; Tagahaya, K.; Nishino, H. *Cancer Lett.* **1997**, *113*, 47−53.

(3) Pérez-Sacau, E.; Díaz-Peñate, R. G.; Estévez-Braun, A.; Ravelo, A. G.; García-Castellano, J.; Pardo, L.; Campillo, M. *J. Med. Chem.* **2007**, *50*, 696−706.

(4) Ríos-Luci, C.; Bonifazi, E. L.; León, L. G.; Montero, J. C.; Burton, G.; Pandiella, A.; Misico, R. I.; Padrón, J. M. *Eur. J. Med. Chem.* **2012**, *53*, 264−274.

(5) da Silva, E. N., Jr; Cavalcanti, B. C.; Guimarães, T. T.; Pinto, M. D. C. F. R.; Cabral, I. O.; Pessoa, C.; Costa-Lotufo, L. V.; de Moraes, M. O.; de Andrade, C. K. Z.; dos Santos, M. R.; de Simone, C. A.; Goulart, M. O. F.; Pinto, A. V. *Eur. J. Med. Chem.* **2011**, *46*, 399−410.

(6) Eyong, K. O.; Kumar, P. S.; Kuete, V.; Folefoc, G. N.; Nkengfack, E. A.; Baskaran, S. *Bioorg. Med. Chem. Lett.* **2008**, *18*, 5387−5390.

(7) Kongkathip, N.; Kongkathip, B.; Siripong, P.; Sangma, C.; Luangkamin, S.; Niyomdecha, M.; Pattanapa, S.; Piyaviriyagul, S.; Kongsaeree, P. *Bioorg. Med. Chem.* **2003**, *11*, 3179−3191.

(8) Zhou, W.; Zhang, X.; Xiao, L.; Ding, J.; Liu, Q.-H.; Li, S.-S. *Eur. J. Med. Chem.* **2011**, *46*, 3420−3438.

(9) Rao, Z.; Liu, X.; Zhou, W.; Yi, J.; Li, S.-S. *Eur. J. Med. Chem.* **2011**, *46*, 3934−3941.

(10) La Ferla, B.; Airoldi, C.; Zona, C.; Orsato, A.; Cardona, F.; Merlo, S.; Sironi, E.; D'Orazio, G.; Nicotra, F. *Nat. Prod. Rep.* **2011**, *28*, 630−648.

(11) Coletti, A.; Lentini, S.; Conte, V.; Floris, B.; Bortolini, O.; Sforza, F.; Grepioni, F.; Galloni, P. *J. Org. Chem.* **2012**, *77*, 6873−6879.

(12) Hashimoto, H.; Saikawa, Y.; Nakata, M. *Pure Appl. Chem.* **2007**, *79*, 507−517.

(13) (a) Sabuzi, F.; Armuzza, V.; Conte, V.; Floris, B.; Venanzi, M.; Galloni, P.; Gatto, E. *J. Mater. Chem. C* **2016**, *4*, 622−629. (b) Bonomo, M.; Sabuzi, F.; Di Carlo, A.; Conte, V.; Dini, D.; Galloni, P. *New J. Chem.* **2017**, *41*, 2769−2779.

(14) Crotti, S.; Posocco, B.; Marangon, E.; Nitti, D.; Toffoli, G.; Agostini, M. *Mass Spectrom. Rev.* **2017**, *36*, 213−251.

(15) Bansal, S.; Bajaj, P.; Pandey, S.; Tandon, V. *Med. Res. Rev.* **2017**, *37*, 404−438.

(16) Connolly, I. D.; Hixson, J. D.; Nagpal, S. *Drugs Future* **2016**, *41*, 731.

(17) Martino, E.; Della Volpe, S.; Terribile, E.; Benetti, E.; Sakaj, M.; Centamore, A.; Sala, A.; Collina, S. *Bioorg. Med. Chem. Lett.* **2017**, *27*, 701−707.

(18) Liu, L. F. *Annu. Rev. Biochem.* **1989**, *58*, 351−375.

(19) Arnò, B.; Coletta, A.; Tesauro, C.; Zuccaro, L.; Fiorani, P.; Lentini, S.; Galloni, P.; Conte, V.; Floris, B.; Desideri, A. *Biosci. Rep.* **2013**, *33*, 269−279.

(20) Botella, P.; Rivero-Buceta, E. *J. Controlled Release* **2017**, *247*, 28−54.

(21) Rio, Y.; Nicoud, J.-F.; Rehspringer, J.-L.; Nierengarten, J.-F. *Tetrahedron Lett.* **2000**, *41*, 10207−10210.

(22) Kimani, S.; Ghosh, G.; Ghogare, A.; Rudshteyn, B.; Bartusik, D.; Hasan, T.; Greer, A. *J. Org. Chem.* **2012**, *77*, 10638−10647.

(23) Emsley, J. *Struct. Bonding. (Berlin)* **1984**, *57*, 147−191.

(24) Iglesias, E. *J. Phys. Chem.* **1996**, *100*, 12592−12599.

(25) Zhu, L.; Wang, W.; Miao, J.; Yin, X.; Hu, X.; Yuan, Y. *J. Mol. Struct.* **2017**, *1141*, 462−468.

(26) Frisch, M. J.; Trucks, G. W.; Schlegel, H. B.; Scuseria, G. E.; Robb, M. A; Cheeseman, J. R.; Scalmani, G.; Barone, V.; Mennucci, B.; Petersson, G. A.; Nakatsuji, H.; Caricato, M.; Li, X.; Hratchian, H. P.; Izmaylov, A. F.; Bloino, J.; Zheng, G.; Sonnenberg, J. L.; Hada, M.; Ehara, M.; Toyota, K.; Fukuda, R.; Hasegawa, J.; Ishida, M.; Nakajima, T.; Honda, Y.; Kitao, O.; Nakai, H.; Vreven, T.; Montgomery, J. A., Jr.; Peralta, J. E.; Ogliaro, F.; Bearpark, M.; Heyd, J. J.; Brothers, E.; Kudin, K. N.; Staroverov, V. N.; Kobayashi, R.; Normand, J.; Raghavachari, K.; Rendell, A.; Burant, J. C.; Iyengar, S. S.; Tomasi, J.; Cossi, M.; Rega, N.; Millam, J. M.; Klene, M.; Knox, J. E.; Cross, J. B.; Bakken, V.; Adamo, C.; Jaramillo, J.; Gomperts, R.; Stratmann, R. E.; Yazyev, O.; Austin, A. J.; Cammi, R.; Pomelli, C.; Ochterski, J. W.; Martin, R. L.; Morokuma, K.; Zakrzewski, V. G.; Voth, G. A.; Salvador, P.; Dannenberg, J. J.; Dapprich, S.; Daniels, A. D.; Farkas, O.; Foresman, J. B.; Ortiz, J. V.; Cioslowski, J.; Fox, D. J. *Gaussian09*, Revision A.02; Gaussian Inc.: Wallingford, CT, 2009.

(27) *Schrödinger*, Release 2016−1: Jaguar, version 9.2; Schrödinger, LLC: New York, NY, 2016.

(28) Galasso, V.; Pichierri, F. *J. Phys. Chem. A* **2009**, *113*, 2534−2543.

(29) Calculated values: ΔG_{solv} (KuQMe) = −18.8843 kcal·mol^{-1}, ΔG_{solv} (NQ)= −19.31284 kcal·mol^{-1}.

(30) Uggerud, E. *Mass Spectrom. Rev.* **1992**, *11*, 389−430.

(31) The gas-phase acidity of a particular species HA is expressed as its heterolytic bond dissociation energy that is equivalent to the proton affinity of A-. See as example: McLuckey, S. A.; Cameron, D.; Cooks, R. G. *J. Am. Chem. Soc.* **1981**, *103*, 1313−1317.

(32) *Gas-Phase Ion Chemistry*; Bowers, M. T., Ed.; Academic: New York, 1979; Vols. *1*−*3*.

(33) Anion proton affinity data are taken from the evaluated database: Bartmess, J. E., Negative Ion Energetics Data, in NIST Chemistry Web Book, *NIST Standard Reference Database Number*, 69 ed.; Linstrom, P. J., Mallard, W. G., Eds.; National Institute of Standards and Technology: Gaithersburg MD, 2005; p 20899 (http://webbook.nist.gov).

(34) Zhao, R.; Al-Said, N. H.; Sternbach, D. L.; Lown, J. W. *J. Med. Chem.* **1997**, *40*, 216−225.

(35) Pallicer, J. M.; Sales, J.; Rosés, M.; Ràfols, C.; Bosch, E. *J. Chromatogr. A* **2011**, *1218*, 6356−6368.

(36) Gottardo, R.; Bertaso, A.; Pascali, J.; Sorio, D.; Musile, G.; Trapani, E.; Seri, C.; Serpelloni, G.; Tagliaro, F. *J. Chromatogr. A* **2012**, *1267*, 198−205.

(37) Martel, S.; Gillerat, F.; Carosati, E.; Maiarelli, D.; Tetko, I. V.; Mannhold, R.; Carrupt, P.-A. *Eur. J. Pharm. Sci.* **2013**, *48*, 21−29.

(38) Sun, J.; Yeung, C. A.; Co, N. N.; Tsang, T. Y.; Yau, E.; Luo, K.; Wu, P.; Wa, J. C.; Fung, K. P.; Kwok, T. T.; Liu, F. *PLoS One* **2012**, *7*, e40720.

(39) Denizot, F.; Lang, R. *J. Immunol. Methods* **1986**, *89*, 271−277.

(40) Bortolini, O.; Nino, A. D.; Eliseo, T.; Gavioli, R.; Maiuolo, L.; Russo, B.; Sforza, F. *Bioorg. Med. Chem.* **2010**, *18*, 6970−6976.

DOI: 10.1021/acs.joc.7b01602
J. Org. Chem. XXXX, XXX, XXX−XXX